Fragmentation of metastable SF6−* ions with microsecond lifetimes in competition with autodetachment

Fragmentation of metastable SF_6^{-*} ions with microsecond lifetimes in competition with autodetachment

K. Graupner,[1] T. A. Field,[1,a)] A. Mauracher,[2] P. Scheier,[2] A. Bacher,[2] S. Denifl,[2] F. Zappa,[2] and T. D. Märk[2]
[1]*Centre for Plasma Physics, School of Mathematics and Physics, Queen's University Belfast, Belfast BT7 1NN, United Kingdom*
[2]*Institut für Ionenphysik und Angewandte Physik, Leopold Franzens Universität, Technikerstrasse 25, A-6020 Innsbruck, Austria*

(Received 26 June 2007; accepted 29 January 2008; published online 11 March 2008)

Fragmentation of metastable SF_6^{-*} ions formed in low energy electron attachment to SF_6 has been investigated. The dissociation reaction $SF_6^{-*} \rightarrow SF_5^- + F$ has been observed $\sim 1.5-3.4$ μs and $\sim 17-32$ μs after electron attachment in a time-of-flight and a double focusing two sector field mass spectrometer, respectively. Metastable dissociation is observed with maximum intensity at ~ 0.3 eV between the SF_6^{-*} peak at zero and the SF_5^- peak at ~ 0.4 eV. The kinetic energy released in dissociation is low, with a most probable value of 18 meV. The lifetime of SF_6^{-*} decreases as the electron energy increases, but it is not possible to fit this decrease with statistical Rice–Ramsperger–Kassel/quasiequilibrium theory. Metastable dissociation of SF_6^{-*} appears to compete with autodetachment of the electron at all electron energies. © *2008 American Institute of Physics*. [DOI: 10.1063/1.2884346]

I. INTRODUCTION

SF_6 is a benchmark molecule for electron attachment; close to zero energy, *s*-wave electron attachment leads to formation of long lived metastable SF_6^{-*} ions. Theoretically, the *s*-wave cross section rises to infinity at zero energy and large experimental cross sections have been reported for SF_6^{-*} formation, e.g., 2×10^3 Å^2 at 1 meV electron energy.[1] The large electron capture cross section and long lifetimes of SF_6^{-*} contribute to the spark suppressing properties of SF_6, which is used extensively as an electrical insulator in high voltage equipment (e.g., Ref. 2). SF_6 is also used in reactive ion etching.[3,4] It is a greenhouse gas and its emission is restricted through the Kyoto protocol.[5] It has been speculated that the potent greenhouse gas SF_5CF_3, recently detected in the atmosphere, is produced by sparks from SF_6 and fluorocarbons in, for example, high voltage applications.[6]

The SF_6^{-*} metastable parent anion can release its excess energy by autodetachment, photon emission, fragmentation, or in collision, as shown here with rate constants k_1-k_4, respectively;

$$SF_6 + e^- \rightarrow SF_6^{-*} \xrightarrow{k_1} SF_6 + e^-, \quad (1)$$

$$SF_6^{-*} \xrightarrow{k_2} SF_6^- + h\nu, \quad (2)$$

$$SF_6^{-*} \xrightarrow{k_3} SF_5^- + F, \quad (3)$$

$$SF_6^{-*} + M \xrightarrow{k_4} SF_6^- + M. \quad (4)$$

Experiments to measure the lifetime of SF_6^{-*} with respect to autodetachment (equivalent to 1/rate, i.e., $1/k_1$) have reported values in the microsecond and millisecond ranges.[7–10] Lifetimes of 10 μs,[7] 25 μs,[8] and 68 ± 2 μs (Ref. 9) have been reported from different mass spectrometry measurements, where autodetachment was observed tens of microseconds after electron attachment. Odom *et al.* observed a range of SF_6^{-*} autodetachment lifetimes from 50 μs to 10 ms in an ion cyclotron resonance experiment; the lifetime measured depended on the experimental observation time, which ranged from ~ 100 μs to 2 ms or more after electron attachment.[10] Odom *et al.* concluded that a range of different states of SF_6^{-*} had been excited with different lifetimes. The excitation of a range of states with different lifetimes implies that experimentally measured lifetime values are averages of all the autodetachment events observed in the experimental time windows. The measurement of average lifetimes explains why mass spectrometric measurements with observation windows tens of microseconds after electron attachment yielded experimental lifetime values in the range of tens of microseconds.

The lifetime of SF_6^{-*} with respect to radiative relaxation $(1/k_2)$ is reported to be in the millisecond range.[10,11] It is not significant here where fragmentation of metastable SF_6^{-*} has been observed with microsecond observation windows.

The only previous direct observations of fragmentation of metastable SF_6^{-*} on microsecond time scales appear to have been the appearance of nonintegral mass peaks in magnetic sector mass spectrometers.[12,13] There was, however, no attempt made to measure lifetimes of the metastable decay in

a)Electronic mail: t.field@qub.ac.uk.

these measurements. Thus, fragmentation of the metastable SF_6^{-*} ion has received little attention, although prompt formation of SF_5^- in dissociative electron attachment has been well studied. The threshold for formation of SF_5^-+F in dissociative electron attachment has been found to be ~0.2 eV electron energy.[14] SF_5^- ions are frequently observed, however, down to 0 eV due to fragmentation of vibrationally excited SF_6^{-*} ions. The high cross section for the formation of SF_6^{-*} close to zero energy can lead to a peak of SF_5^- at zero with an intensity that depends strongly on the temperature of the sample.[14,15] A second SF_5^- peak is usually observed above threshold with a maximum at 0.3–0.6 eV.[1,14,16,17] It has been suggested that the high energy side of this second peak is limited by the decrease in the *s*-wave attachment cross section with increasing electron energy, and low energy side of the peak is limited by the dissociation threshold (see, for example, Ref. 18). The variation in the position of the maximum between 0.3 and 0.6 eV may also be due to differences in gas temperature.

This investigation of fragmentation of metastable SF_6^{-*} was inspired by the recent work of Braun *et al.*,[16,17] which suggests that the electron attachment resonance responsible for the formation of SF_6^- close to zero electron energy also leads to the formation of SF_5^-[16] and that SF_5^- is also formed by direct dissociation over a repulsive electronic state.[17]

In part of the present work, dissociation of SF_6^{-*} was observed ~1.5–3.4 μs after electron attachment and it was, thus, expected that lifetimes of a few microseconds would be observed because of the conclusion of Odom *et al.* that experimentally observed lifetime values depend on the observation time window.[10] A new feature of the present work, however, is the measurement of SF_6^{-*} lifetimes as a function of electron energy and, hence, as a function of SF_6^{-*} internal energy. The internal energy of SF_6^{-*} formed in electron attachment is, of course, equal to the electron energy plus the electron affinity and initial internal energy of SF_6. Dissociation of SF_6^{-*} ions has also been observed at longer times after electron attachment, and the kinetic energy released is measured in this work to deduce more information about the dissociation of SF_6^{-*}.

II. EXPERIMENTS

A time-of-flight mass spectrometer in Belfast and a double focusing two sector field mass spectrometer in Innsbruck have been used to observe the fragmentation of metastable SF_6^{-*} to form SF_5^-+F. The time-of-flight mass spectrometer is part of the electron radical interaction chamber (ERIC), which has been described previously.[19] Briefly, negative ions are produced by collisions with slow electrons from a trochoidal monochromator with an energy resolution of ~250 meV, determined from the width of the SF_6^- signal at zero energy (full width at half maximum). The experiment is pulsed at ~12 kHz. Ions are generated in a 1 μs electron beam pulse and accelerated from the interaction region with a repeller pulse, which is applied 1 μs after the end of the electron pulse. The repeller pulse is delayed to ensure all electrons have left the interaction region before the ions are extracted into the time-of-flight mass spectrometer.

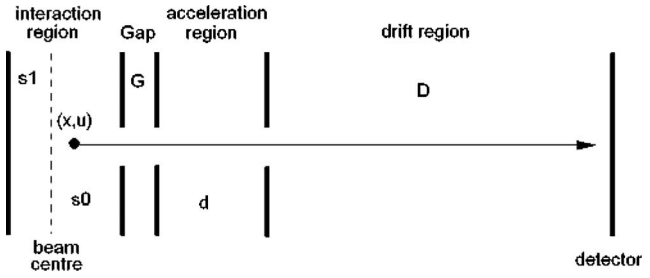

FIG. 1. Schematic diagram to show the geometry of the mass spectrometer.

A schematic diagram of the time-of-flight mass spectrometer is shown in Fig. 1. Ions are accelerated in the interaction region, when the repeller pulse is applied, and in the acceleration region, but the gap and drift region are field-free. Typically, the time of flight of ions is proportional to the square root of their mass. By contrast, in "metastable dissociation" events, where SF_6^{-*} ions dissociate into SF_5^- ions while they are being accelerated, the time of flight will have an intermediate value between the flight times of SF_5^- and SF_6^{-*}. Figure 2 shows experimental and Monte Carlo simulated mass spectra with the characteristic signature of metastable dissociation events in between mass peaks due to SF_5^- and SF_6^{-*} ions.

Zones 1 and 2 in Fig. 2 correspond to metastable dissociation in the interaction and acceleration regions, respectively. If metastable dissociation occurs in the interaction region just after the repeller pulse is applied, then the speed of the SF_5^- ion entering the drift region will be slightly slower than the typical speed of SF_5^- ions and the time of flight observed will be close to the typical flight time of SF_5^- ions. Thus, metastable dissociation in the interaction region in zone 1 is close to the SF_5^- peak in the time-of-flight mass spectrum. By contrast, if a SF_6^{-*} ion dissociates close to the end of the acceleration region, the time of flight observed will be close to typical values for SF_6^{-*} and zone 2 is adjacent to the SF_6^{-*} peak. Indeed, the exact time of flight observed depends on the position, and hence time, of dissociation. The intensity in zone 2 is weaker than in zone 1 because ions are accelerated twice as quickly in the acceleration region, as in the interaction region and the metastable signal is spread more thinly. Visible in Figs. 2(a), 2(b), and 2(d) is a slight hump or peak in between zones 1 and 2 due to dissociation in the field-free gap; the experimental signal-to-noise ratio in Fig. 2(c) is insufficient for the observation of this feature. The time spent by SF_6^{-*} ions in the interaction region is ~1.2 μs, in the gap it is ~60 ns, and it is ~0.6 μs in the acceleration region. Thus, the observation window in the time-of-flight measurements for metastable dissociation is ~1.5–3.4 μs by the addition of the average delay between electron attachment and the start of the repeller pulse 1.5 μs to the flight time window of 0–1.9 μs.

The two sector field mass spectrometer (VG ZAB-2SEQ) has also been described previously.[20] Negative ions are produced in a collision chamber, heated to 200 °C to avoid contamination, by low energy electrons with an energy resolution of ~1 eV. Ions are accelerated to 7 keV kinetic energy and mass selected with a magnetic sector. Se-

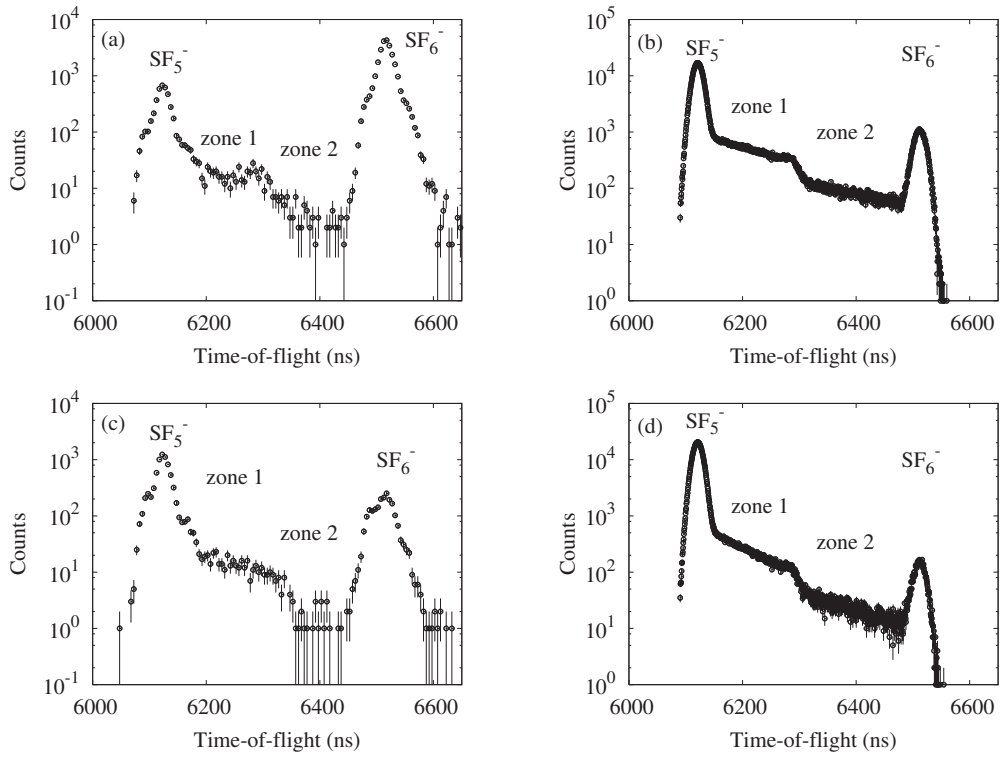

FIG. 2. Time-of-flight spectra of metastable dissociation $SF_6^{-*} \rightarrow SF_5^- + F$. Experimental data at (a) 0.24 eV and (c) 0.44 eV, and Monte Carlo simulations with lifetimes of (b) 1150 ns and (d) 650 ns. Dissociation in the interaction region, acceleration region, and the gap is observed in zone 1, zone 2, and the small hump between zones 1 and 2, respectively.

lected ions pass along a ~1.5 m field-free region to the electric sector. Fragment ions formed in the field-free region by metastable dissociation will, of course, have lower kinetic energies than undissociated parent ions and can be observed by scanning the pass energy of the electric sector; this scan yields a mass-analyzed ion kinetic energy (MIKE) spectrum. The distribution of kinetic energies released in dissociation can be determined from the shape of metastable peaks in MIKE spectra.[21] In this work, SF_6^{-*} ions passed through the field-free region from ~17 to 32 μs after electron attachment. Autodetachment of metastable ions can also be observed in a second field-free region between the electric sector and the secondary electron multiplier where ions are detected. If ions are deflected halfway along this region, then only fast neutrals formed by autodetachment between the electric sector and the ion deflector will be detected with the electron multiplier; the ratio of the undeflected to deflected count rate can be used to determine the rate of autodetachment and, hence, the lifetime of metastable ions in this region. Here the time SF_6^{-*} ions passed along the second field-free region was from ~38 to 40 μs after electron attachment.

III. RESULTS AND ANALYSIS

A. Time-of-flight data

A spectrum of dissociative electron attachment to SF_6 observed with ERIC is shown in Figs. 3(a) and 3(b) with logarithmic and expanded linear intensity scales. The abscissa is ion flight time, and the flight times of SF_5^- and SF_6^- ions are indicated above the upper abscissa. The positions of

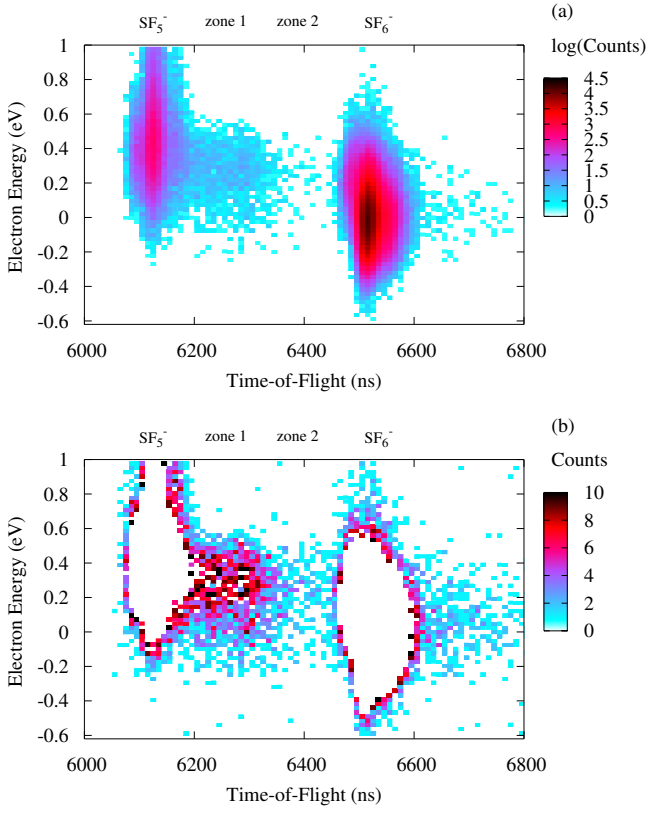

FIG. 3. (Color online) Two-dimensional spectrum of electron attachment to SF_6. The ion intensity is represented with (a) logarithmic grayscale and (b) expanded linear grayscale. In (b), white points indicate either zero counts or more than ten counts. The metastable signal in zones 1 and 2 is clearer in (b).

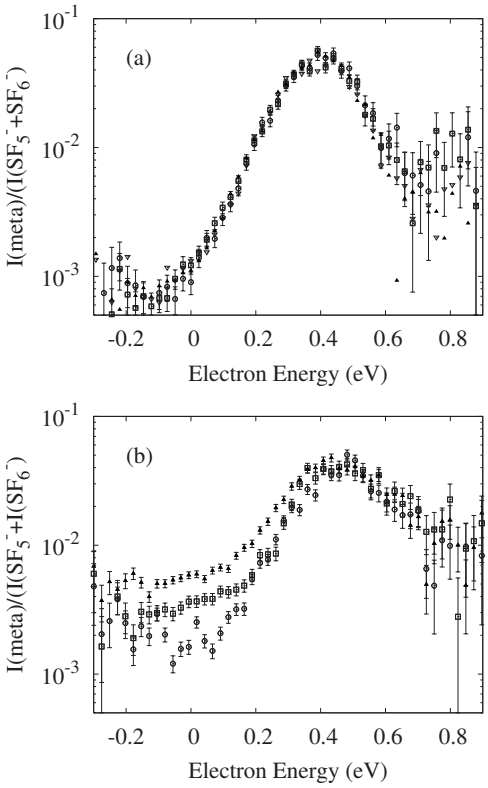

FIG. 4. Ratio of total metastable intensity to $SF_5^-+SF_6^-$ intensity at (a) low and (b) high pressures. In (a), there is no pressure dependence of the ratio, while in (b), the ratio is pressure dependent. Relative pressures in (a) 1 (○): 2 (□): 3 (▲): 4 (▽). Relative pressures in (b) 1 (○): 1.4 (□): 3 (▲).

zones 1 and 2, discussed above with Fig. 2, are also indicated in Fig. 3. The ordinate is electron energy; in effect, each horizontal line of Fig. 3 represents a time-of-flight mass spectrum similar to those shown in Fig. 2 recorded at the electron energy indicated on the ordinate. Peaks are visible for the prompt formation of SF_5^- and SF_6^{-*} in the interaction region, and the metastable signal is visible in zones 1 and 2.

An alternative explanation for the signal in zones 1 and 2 is that it arises due to collisional dissociation of SF_6^{-*} by, for example, the process

$$SF_6^{-*} + SF_6 \rightarrow SF_5^- + F + SF_6, \tag{5}$$

which has been observed previously.[22] Measurements were made at many different gas pressures to determine if there were any contribution from collisional processes. The results are shown in Figs. 4(a) and 4(b). In Fig. 4(a), the ratio of metastable signal to $SF_5^-+SF_6^-$ signal is plotted against electron energy for four gas inlet pressures, with the pressure ratios 1: 2: 3: 4; the results are independent of pressure within the experimental uncertainty. In Fig. 4(b), the pressures are higher by an order of magnitude or more and the ratio of metastable to $SF_5^-+SF_6^-$ signal is clearly dependent on the pressure. All the results presented here were taken under the collision-free conditions of Fig. 4(a), where purely metastable dissociation is observed.

Integrated signals of SF_6^- and SF_5^- and metastable signal are shown in Fig. 5 as a function of electron energy. The SF_6^- peak position was used to determine the position of zero electron energy. The position of the SF_5^- maximum observed

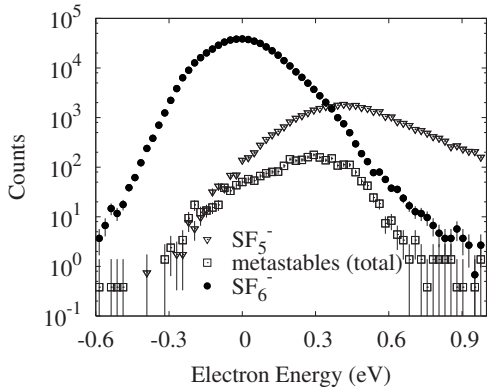

FIG. 5. Integrated intensities of SF_6^{-*} and SF_5^-, and metastable fragmentation signal from zones 1 and 2 as a function of electron energy. The peak of SF_6^{-*} was used to determine the position of 0 eV. SF_5^- has its maximum at 0.4 eV and the maximum of the total metastable intensity appears at ~0.3 eV. Background has been subtracted.

here, 0.4 eV, is within the range of previously reported values. The peak of metastable signal, ~0.30 eV, lies close to the point at which the intensities of SF_6^- and SF_5^- are equal, ~0.35 eV. This position of the metastable peak in between the SF_6^- and SF_5^- maxima suggests that with increasing electron energy, the lifetime of SF_6^{-*} ions decreases. A logarithmic vertical scale is used in Fig. 5 because of the large range of intensities displayed. The electron energy resolution here, 250 meV, may account for the observation of metastable signal down to zero eV, which is below the threshold for SF_5^- formation, ~0.2 eV.[14]

Simulated time-of-flight mass spectra of metastable dissociation have been generated with a Monte Carlo simulation to compare with experimental spectra. The trajectories of a million SF_6^{-*} ions were calculated for each simulated mass spectrum with the assumptions that the gas temperature was 300 K and that all SF_6^{-*} ions dissociate exponentially with a single lifetime to give SF_5^-+F. Additionally, a random delay of between 1 and 2 μs was included to take account of the time between electron attachment and the application of the repeller pulse. Simulated mass spectra are shown above in Figs. 2(b) and 2(d) with experimental spectra in Figs. 2(a) and 2(c).

Quantitative lifetimes of metastable SF_6^{-*} ions have been estimated by comparison of the experimental spectra with simulated spectra and the assumption that loss of SF_6^{-*} is well represented by a single exponential. The fraction of the total metastable intensity located in zone 1, $F_{\mathrm{exp,sim}}$, has been calculated with

$$F_{\mathrm{exp,sim}} = \frac{I(\text{zone 1})}{I(\text{zone 1}) + I(\text{zone 2})} \tag{6}$$

for both experimental and simulated spectra, where $I(\text{zone } i)$ is the metastable intensity in zone i. This fraction depends on the lifetime of SF_6^{-*}, as shown in Fig. 6, where the fractions of simulated mass spectra, F_{sim}, are plotted against the lifetimes used to generate them. Figure 6 also shows a rational function of degree 2, which was fitted to these points; this function was used to convert experimental fractions F_{exp} into lifetimes. The intensities used to determine fractions have

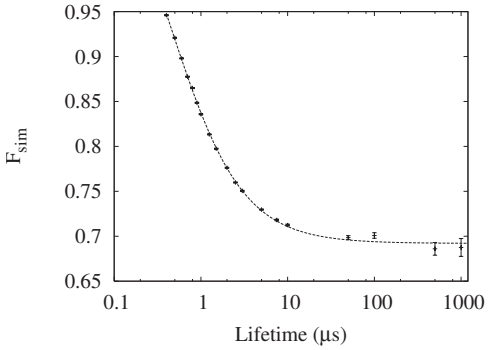

FIG. 6. Fractions of the total metastable intensity located in zone 1 of simulated mass spectra, F_{sim}, plotted against the lifetime used to generate the simulated spectrum.

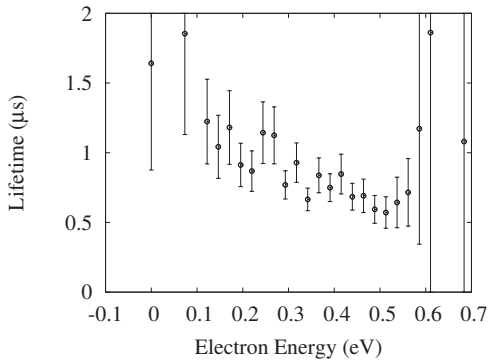

FIG. 8. SF_6^{-*} lifetimes as a function of electron energy determined from experimental fractions, F_{exp}. Lifetimes in the region 0.1–0.5 eV are reliable; outside this region, the error bars reflect the weakness of the metastable signal and can be so large that they cannot be plotted on the vertical scale.

been determined carefully to avoid any contributions from the extra intensity between zones 1 and 2 due to the gap and the mass peaks of SF_6^-, SF_5^-, and $^{34}SF_5^-$; furthermore, identical procedures were used to calculate the intensities from simulated and experimental data. For lifetimes beyond ~ 10 μs, the fraction approaches a lower limit of 0.7 because it is impossible to distinguish longer lifetimes with the experimental observation window of $\sim 1.5-3.4$ μs.

Figure 7 shows the experimental fractions of the metastable signal in zone 1, F_{exp}. These fractions have been converted into the lifetimes shown in Fig. 8, with the function shown in Fig. 6. A clear tendency towards shorter lifetimes with increasing electron energy is observed.

The simulated spectra shown in Figs. 2(b) and 2(d) were calculated with lifetimes of 1150 and 650 ns, which are the best fit lifetimes for the experimental data at 0.24 and 0.44 eV shown in Figs. 2(a) and 2(c), respectively. The agreement between experimental and simulated data is reasonable in zones 1 and 2. The relative integrated intensities of the SF_5^- peaks above the metastable signal in the simulated and experimental spectra agree to within 25% in the data shown in Fig. 2. Statistical analysis of all the experimental and simulated spectra between 0.1 and 0.5 eV reveals that the ratio of experimental SF_5^- intensity to simulated SF_5^- intensity is 1.0 ± 0.3, where the uncertainty represents one standard deviation. The SF_6^{-*} peak, however, is noticeably smaller in both simulated spectra than in the experimental spectra. This discrepancy in the SF_6^{-*} peak height is expected

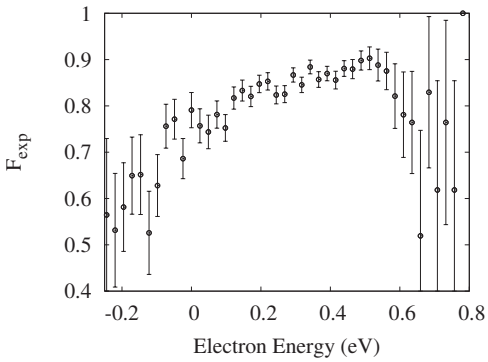

FIG. 7. Experimental fractions of the total metastable intensity located in zone 1, F_{exp}, as a function of electron energy.

because of the different processes that contribute to, on the one hand, the SF_6^{-*} peak and, on the other hand, the SF_5^- peak and the metastable signal in zones 1 and 2.

Four processes for loss of SF_6^{-*} are described in Sec. I; autodetachment with rate constant k_1, photon emission k_2, fragmentation k_3, and collision k_4. As discussed in Sec. I, the rate of photon emission is insignificant here so k_2 will not be considered further. Furthermore, the data were recorded under collision-free conditions so k_4 will not be considered either. Therefore, autodetachment and fragmentation with rate constants k_1 and k_3 determine the rate of loss of SF_6^{-*} in this experiment. Assuming simple exponential behavior, k_1 and k_3 are rational numbers and the population of SF_6^{-*}, $N_{SF_6^{-*}}(t)$, will be given by

$$N_{SF_6^{-*}}(t) = N_{SF_6^{-*}}(0)e^{-(k_1+k_3)t}, \tag{7}$$

where $N_{SF_6^{-*}}(0)$ is the initial population of metastable SF_6^{-*} ions. Thus, the lifetime of SF_6^{-*}, $\tau_{SF_6^{-*}}$, is given by

$$\tau_{SF_6^{-*}} = \frac{1}{k_1 + k_3}. \tag{8}$$

The fraction of SF_6^{-*} ions that fragment to form SF_5^-, $\lambda_{SF_5^-}$, is given by

$$\lambda_{SF_5^-} = \frac{k_3}{k_1 + k_3} \tag{9}$$

and, hence, the population of SF_5^- ions formed in fragmentation, $N_{SF_5^-}(t)$, is given by

$$N_{SF_5^-}(t) = \lambda_{SF_5^-} N_{SF_6^{-*}}(0)(1 - e^{-(k_1+k_3)t}). \tag{10}$$

An assumption of the Monte Carlo simulation was that SF_6^{-*} ions can fragment to give SF_5^-, but do not autodetach. A consequence of this assumption is that the relative intensities of the SF_5^- peak and the metastable intensity in zones 1 and 2 are too large by a factor of $1/\lambda_{SF_5^-}$; the only part of the spectrum that is not too large is the SF_6^{-*} ion peak, which, therefore, appears to be too small in the simulated spectra in Figs. 2(b) and 2(d) compared to the experimental spectra in Figs. 2(a) and 2(c). It is possible from the difference in the relative intensities of the SF_6^{-*} peaks in the simulated and

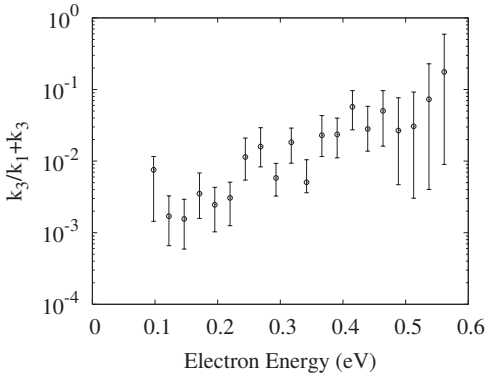

FIG. 9. Estimates of $\lambda_{SF_5^-}=k_3/k_1+k_3$ (see text).

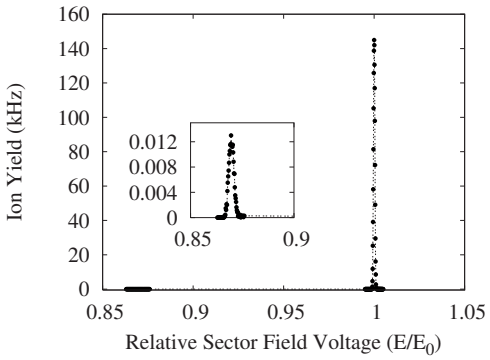

FIG. 11. MIKE spectrum showing a strong SF_6^{-*} parent ion signal and a weak metastable due to loss of 19 Thompson, i.e., $SF_6^{-*} \rightarrow SF_5^- + F$.

experimental spectra to make a quantitative estimate of the branching fraction $\lambda_{SF_5^-}$; Fig. 9 shows estimates of this branching fraction as a function of incident electron energy.

It is straightforward to show from Eqs. (8) and (9) that the individual rates of autodetachment (k_1) and fragmentation (k_3) of SF_6^{-*} are given by

$$k_1 = \frac{1-\lambda_{SF_5^-}}{\tau_{SF_6^{-*}}}, \tag{11}$$

$$k_3 = \frac{\lambda_{SF_5^-}}{\tau_{SF_6^{-*}}}. \tag{12}$$

Figure 10 shows estimates of the lifetimes of SF_6^{-*} ions with respect to autodetachment, equivalent to $1/k_1$, and dissociation, $1/k_3$, which were calculated with Eqs. (11) and (12). The size of the error bars of the lifetimes reflects the uncertainties in the values of $\tau_{SF_6^{-*}}$ and $\lambda_{SF_5^-}$ shown in Figs. 8 and 9.

B. Two sector field data

A MIKE scan for metastable dissociation of SF_6^{-*} in the field-free region between the magnetic and electric sectors of the double focusing mass spectrometer is shown in Fig. 11. A small metastable peak is observed due to the formation of SF_5^- with an intensity $\sim 10^4$ times smaller than the parent ion peak. The reason for the weakness of the metastable peak is not certain. It may be that only a small proportion of the SF_6^{-*} ions in the beam have sufficient internal energy to dissociate, and another factor may be that the rate of dissociation could be slow for those ions.

The kinetic energy released in the metastable dissociation determined from the MIKE scan is shown in Fig. 12; the most probable kinetic energy release is ~18 meV and there is little intensity above 50 meV.

The autodetachment (autoneutralization) lifetime of the SF_6^{-*} measured in the second field-free region between the electric sector and the ion detector was found to be ~93 μs, with an observation window of 38–40 μs.

IV. DISCUSSION

The results of the time-of-flight and two sector field mass spectrometric measurements are consistent. The time-of-flight measurements indicate that the lifetimes of SF_6^{-*} ions become shorter as the electron impact energy increases. For example, above 0.3 eV electron energy, i.e., 0.1 eV higher than the SF_5^- threshold, the measured SF_6^{-*} lifetimes are all below 1 μs. These measurements predict that in the two sector field mass spectrometer, where fragmentation is observed between ~17 and 32 μs after electron attachment, only SF_6^{-*} ions with internal energies just above the dissociation threshold will be present because higher energy SF_6^{-*} ions formed in the ion source will have already dissociated.

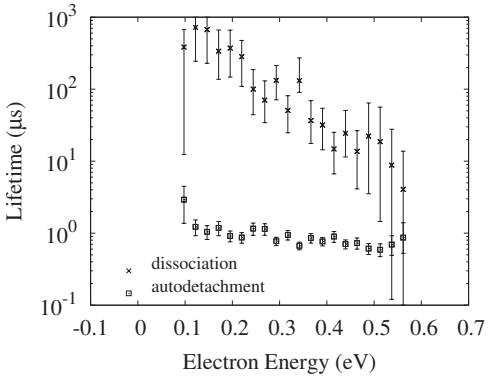

FIG. 10. Estimates of autodetachment and dissociation lifetimes ($1/k_1$ and $1/k_3$) calculated from $\tau_{SF_6^{-*}}$ and $\lambda_{SF_5^-}$ (see text).

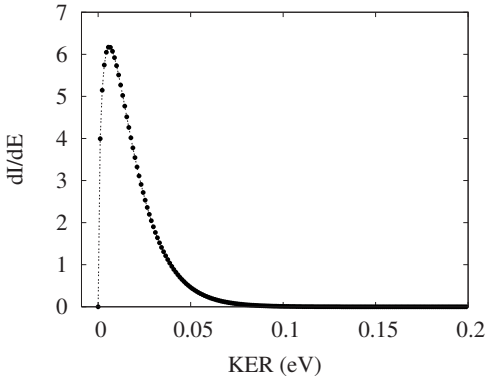

FIG. 12. Kinetic energy released in the reaction $SF_6^{-*} \rightarrow SF_5^- + F$ determined from the metastable peak in the MIKE spectrum.

The low kinetic energy released in dissociation, with a maximum at 18 meV, is consistent with this prediction.

An unexpected observation from the present data is that all of the SF_5^- signals observed between 0.1 and 0.5 eV can be accounted for by metastable dissociation of SF_6^{-*}. SF_5^- fragment ion peaks are observed in the Monte Carlo simulated data, visible in Fig. 2, due to dissociation of SF_6^{-*} ions during the 1–2 μs delay between electron attachment and the application of the drawout pulse. The intensities of the SF_5^- peaks in the simulated spectra match the experimentally observed SF_5^- intensities to within ±30% (standard deviation) between 0.1 and 0.5 eV. Therefore, the formation of SF_5^- in fast dissociation events below 0.5 eV electron impact energy is at most a minor dissociation channel compared to metastable dissociation with microsecond lifetimes.

There has been some discussion as to whether SF_6^{-*} and SF_5^- are formed following two different electron attachment processes to SF_6 or whether the same electron attachment process leads to the formation of both SF_6^{-*} and SF_5^- ions (see Refs. 16 and 17, and references therein). It is clear from the present measurements that both SF_6^{-*} ions and SF_5^- ions are formed from the same electron attachment process. It is also clear from the present comparison of the Monte Carlo simulations with experimental data that any additional electron attachment process that leads to the formation of SF_5^- ions only is at most a weak channel compared to the formation of metastable SF_6^{-*} ions, which fragment to give SF_5^-. Indeed, the present experimental data can be explained by a single electron attachment process that leads to the formation of metastable SF_6^{-*} ions close to zero electron energy. It is not possible from the present data, however, to rule out the possibility that there is more than one electron attachment process close to zero electron energy, which leads to the formation of SF_6^{-*}, SF_5^-, or both ions.

The overall picture that emerges of the behavior of SF_6^{-*} formed in electron attachment to SF_6 is that above the threshold for dissociation, there is competition between loss of an electron in autodetachment and fragmentation of the molecule on the microsecond time scale. The rates of autodetachment and fragmentation depend critically on the internal energy of the SF_6^{-*} ion. Close to the threshold for dissociation, the rate of fragmentation is orders of magnitude slower than the rate of autodetachment, but the rate of fragmentation approaches the rate of autodetachment as the internal energy of the SF_6^{-*} ion increases.

Attempts have been made to fit the variation in SF_6^{-*} lifetime as a function of electron energy observed here with Rice–Ramsperger–Kassel (RRK)/quasiequilibrium theory (QET) statistical theory, but it has not been possible to do this. It has also not been possible to fit the individual rates of autodetachment and fragmentation with statistical theory. It is not clear why these fits have not been possible, but it may be because with seven atoms, SF_6^{-*} is not large enough for this elementary statistical theory to model the fragmentation dynamics. Quantum mechanical calculations of electron attachment to SF_6 based on Gauyacq and Herzenberg's model[23] have recently been performed by Gerchikov and Gribakin with consideration of the nuclear motion and vibrational energy redistribution (IVR).[24] They conclude that vibrational energy redistribution in SF_6^- is very efficient, which accounts for the large autodetachment lifetimes observed in the millisecond range. Furthermore, these calculations also predict nonexponential decay in autodetachment.

The competition between loss of an electron and fragmentation of the SF_6^{-*} molecular ion may be an interesting theoretical challenge to model. Slow metastable fragmentation of positively charged molecular ions is well known, e.g., Ref. 25. Delayed ionization of C_{60}, for example, has been observed,[26] where an electron is ejected from a vibrationally excited C_{60} molecule on the microsecond time scale, but this may be one of the first times that competition between slow fragmentation and slow loss of an electron has been observed, where slow refers to time scales that are orders of magnitude longer than molecular vibrational periods.

V. CONCLUSIONS

Fragmentation of metastable SF_6^{-*} ions, formed by electron attachment to SF_6, into SF_5^-+F has been investigated with a time-of-flight and a two sector field mass spectrometer. Metastable fragmentation between ~1.5 and 3.4 μs after electron attachment was observed in the time-of-flight mass spectrometer with electron impact energies of ~0.5 eV down to the threshold for formation of SF_5^-, with maximum intensity at ~0.30 eV. Time-of-flight spectra have been compared with Monte Carlo simulated spectra to determine lifetimes of SF_6^{-*} ions at each electron impact energy; the lifetimes of SF_6^{-*} ions decrease with increasing electron energy, but it has not been possible to fit the data with RRK/QET statistical theories. A MIKE spectrum of SF_6^{-*} fragmentation in the two sector field mass spectrometer ~17–32 μs after electron attachment shows a weak metastable signal four orders of magnitude weaker than the parent ion peak. The kinetic energy released in dissociation determined from the MIKE spectrum was small, with a most probable energy release of 18 meV. Autodetachment of SF_6^{-*} was also observed directly in the two sector field mass spectrometer ~38–40 μs after electron attachment.

It is concluded that there is competition between fragmentation and autodetachment of an electron in SF_6^{-*} ions with sufficient internal energy to dissociate. The present data can be accounted for by a single process of electron attachment to SF_6 close to zero electron energy responsible for the formation of SF_6^{-*}, which can autodetach or dissociate to give SF_5^-+F. The possibility that additional electron attachment processes contribute to the formation of SF_6^{-*} and/or SF_5^- close to zero energy cannot be ruled out.

ACKNOWLEDGMENTS

K.G. is grateful to the European Social Fund (ESF) for providing a Ph.D. studentship. The authors also gratefully acknowledge financial support from the EPSRC (GR/N04362/2), the Royal Society (RSRG 21245), and the European Science Foundation (ESF) network EIPAM. This work is partially supported by the FWF, Wien and the European Commission, Brussels.

[1] L. G. Christophorou and J. K. Olthoff, J. Phys. Chem. Ref. Data **29**, 267 (2000).
[2] F. Buret and A. Beroual, IEEE Trans. Power Deliv. **11**, 267 (1996).
[3] X. Li, T. Abe, and M. Esashi, Sens. Actuators, A **87**, 139 (2001).
[4] M. A. R. Alves, L. F. Porto, P. H. L. de Faria, and E. S. Braga, Vacuum **72**, 485 (2004).
[5] Document No. FCCC/CP/1997/7/Add.1, available on http://www.unfccc.int.
[6] L. Huang, L. Zhu, X. Pan, J. Zhang, B. Ouyang, and H. Hou, Atmos. Environ. **39**, 1641 (2005).
[7] D. Edelson, J. E. Griffiths, and K. B. McAfee, J. Chem. Phys. **37**, 917 (1962).
[8] R. N. Compton, L. G. Christophorou, G. S. Hurst, and P. W. Reinhardt, J. Chem. Phys. **45**, 4634 (1966).
[9] P. W. Harland and J. C. J. Thynne, J. Phys. Chem. **75**, 3517 (1971).
[10] R. W. Odom, D. L. Smith, and J. H. Futrell, J. Phys. B **8**, 1349 (1975).
[11] M. S. Foster and J. L. Beauchamp, Chem. Phys. Lett. **31**, 482 (1975).
[12] C. Lifshitz, A. M. Peers, R. Grajower, and M. Weiss, J. Chem. Phys. **53**, 4605 (1970).
[13] A. J. Ahearn and N. B. Hannay, J. Chem. Phys. **21**, 119 (1953).
[14] C. Chen and P. Chantry, J. Chem. Phys. **71**, 3897 (1979).
[15] D. Smith, P. Spanel, S. Matejcik, A. Stamatovic, T. D. Märk, T. Jaffke, and E. Illenberger, Chem. Phys. Lett. **240**, 481 (1995).
[16] M. Braun, M.-W. Ruf, H. Hotop, and M. Allan, Chem. Phys. Lett. **419**, 517 (2006).
[17] M. Braun, F. Gruber, M.-W. Ruf, S. V. K. Kumar, E. Illenberger, and H. Hotop, Chem. Phys. **329**, 148 (2006).
[18] S. Matejcik, P. Eichberger, B. Plunger, A. Kiendler, A. Stamatovic, and T. D. Märk, Int. J. Mass Spectrom. Ion Process. **114**, L13 (1995).
[19] T. A. Field, A. E. Slattery, D. J. Adams, and D. D. Morrison, J. Phys. B **38**, 255 (2005).
[20] D. Huber, M. Beikircher, S. Denifl, F. Zappa, S. Matejcik, A. Bacher, V. Grill, T. D. Märk, and P. Scheier, J. Chem. Phys. **125**, 084304 (2006).
[21] J. H. Beynon and R. G. Cooks, J. Phys. E **7**, 10 (1974).
[22] J. P. McGeehan, B. C. O'Neill, A. N. Prasad, and J. D. Craggs, J. Phys. D **8**, 153 (1975).
[23] J. P. Gauyacq and A. Herzenberg, J. Phys. B **17**, 1155 (1984).
[24] L. G. Gerchikov and G. F. Gribakin, "Electron attachment to SF_6 and lifetimes of SF_6^- negative ions," Phys. Rev. A (submitted).
[25] R. G. Cooks, J. H. Beynon, R. M. Caprioli, and R. G. Lester, *Metastable Ions* (Elsevier, Amsterdam, 1973).
[26] E. E. B. Campbell, G. Ulmer, and I. V. Hertel, Phys. Rev. Lett. **67**, 1986 (1991).